

## **Risk Analysis and Simulation for Geologic Storage of CO<sub>2</sub>**

\*Kwang-Seok Chae<sup>1)</sup> and Jea-woo Lee<sup>2)</sup>

<sup>1)</sup> *Infra & Offshore Research Team, GS Engineering & Construction, Korea,*

<sup>2)</sup> *WorleyParsons PTY, Melbourne, Australia*

<sup>1)</sup> [kschae@gconst.co.kr](mailto:kschae@gconst.co.kr)

### **ABSTRACT**

Carbon capture and sequestration (CCS) is a promising way for long term storage of carbon-dioxide (CO<sub>2</sub>). The analysis of CO<sub>2</sub> injection and potential leakage scenarios is usually associated with large underground reservoirs. The task of certifying reservoirs for CO<sub>2</sub> storage is complex and requires the identification of potential leakage of CO<sub>2</sub> and brine from storage formations. Wellbores (abandoned and in use), faults, and fractured caprock are common leakage pathways that present risk factors for CCS. The objective of this paper is to simulate CO<sub>2</sub> injection and subsequent transport under different possible scenarios for the purpose of sequestration. We have used the Finite Element Heat Mass (FEHM) code to perform the simulations, including simulations of possible leakage pathways. In addition, we demonstrated a coupling of FEHM with the Goldsim software for probabilistic analysis.

### **1. INTRODUCTION**

Geologic sequestration of carbon-dioxide (CO<sub>2</sub>) is being studied as a promising way for long term storage of CO<sub>2</sub>. The task of certifying reservoirs for CO<sub>2</sub> storage is complex and requires, among many other tasks, the assessment of potential risks of leakage of CO<sub>2</sub> and brine from storage formations (mature oil reservoirs, or aquifers with poor water quality and high salinity) into drinking water aquifers. Wellbores (abandoned and in use), faults, and fractured caprock are possible leakage paths that present risk factors for carbon capture and sequestration (CCS). When anticipating injecting large amounts of CO<sub>2</sub> into oil reservoirs, wellbore leakage paths are especially important because of the large number of wells tapping the reservoirs. Past studies have shown that wellbore annulus can also be important because of the interaction between CO<sub>2</sub>-rich water and cement. Thus three typical leakage pathways comprising wellbores, faults, and fractured/semi-permeable caprock, are the primary focus in the current study scope.

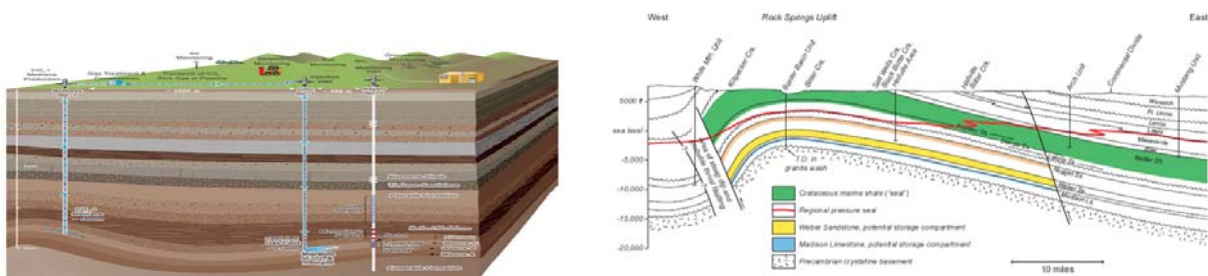
The analysis of CO<sub>2</sub> injection and potential leakage scenarios is usually associated with a large underground reservoir. This potential storage site may be a relatively deep brine aquifer or an active or abandoned oil and/or gas reservoir. Figure 1 shows two of

---

<sup>1), 2)</sup> Ph.D.

the many sites that are being considered for CO<sub>2</sub> sequestration, illustrating the typical settings. Figure 1(a) shows a cross section of the Otway Basin in Southern Australia; a depleted gas reservoir. The cross section shows the complex stratigraphic sequence and the positions where the CO<sub>2</sub> injection and monitoring wells are located. Figure 1(b) (Sharma 2009) shows the Rock Springs Uplift in Wyoming, United States of America which is a potential storage site for CO<sub>2</sub> captured from a nearby coal-fired power plant.

Recent advances in modern computers and numerical algorithms have facilitated explicit simulation of entire reservoirs spreading over tens to hundreds of square kilometers. This large-scale regional approach to CO<sub>2</sub> sequestration modeling is often needed for reservoir management including planning of drilling programs and coordination with surface facilities. However, seeing that leakage is a local-scale phenomenon associated with small scale features and properties in which steep gradients are expected, the evaluation of CO<sub>2</sub> storage and leakage needs a more local and detailed description of the reservoir and wellbore.



(a) Cross section of Otway Basin (b) Rock Springs Uplift in Wyoming  
 Fig. 1 Examples of sites considered for CO<sub>2</sub> sequestration

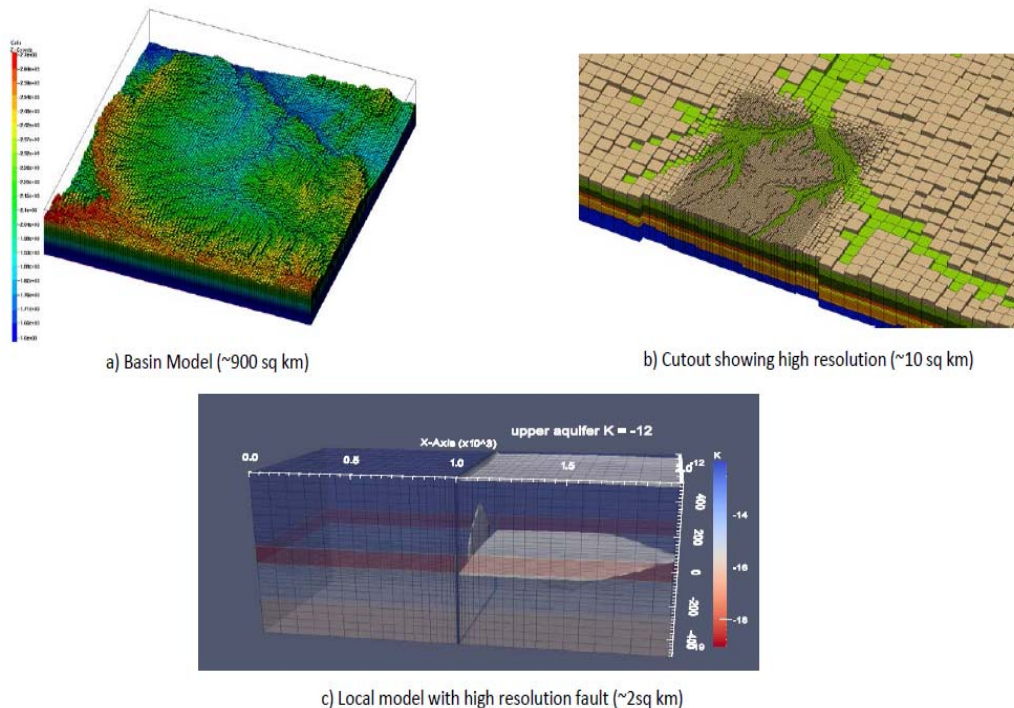


Fig. 2 Example of large scale reservoir model with an embedded high resolution model

The separate goals of reservoir management and CO<sub>2</sub> storage and leakage evaluation can both be met by using a large scale reservoir model with an embedded high resolution model as illustrated Figure 2. The number of grid-blocks for each model is roughly 1 million, 400 thousand, and 22 thousand for the 900 square kilometers (km<sup>2</sup>) basin model, the 10 km<sup>2</sup> intermediate scale model, and the 2 km<sup>2</sup> local model, respectively. The local model is truncated not only in the horizontal directions but also in the vertical direction allowing for higher resolution near the boundaries of the caprock, where steep pressure gradients are expected. Numerical errors caused by an inadequate numerical grid (e.g. numerical dispersion) can be avoided with an adequate resolution achieved by testing the local models. Thus, the ability of the selected software to conduct both regional-scale and local-scale simulation is an important selection criterion.

The majority of published studies have utilized two dimensional (2D) or axisymmetric models to address wellbore leakage cases. However, since three dimensional (3D) models are apparently suited to realistic simulations, this study was intended to develop 3D models to take into account three dimensional effects such as cross-formational (lateral) groundwater flow (cross flow) in receiving aquifers including point sources for the wellbore leakage case, realistic plumes from point sources (inherently 3D) for the caprock leakage case, and non-uniform fault flow for the fault leakage case. To this end, 3D simulation capability was another important software selection criterion.

While there has been much research on the use of injected CO<sub>2</sub> to increase the productivity of oil reservoirs, the use of oil reservoirs as either primarily CO<sub>2</sub> sequestration sites or as dual-use sites for enhanced oil recovery and CO<sub>2</sub> storage, has received far less attention. An area of concern is the lack of information on reservoir behavior from fluid, geochemical, and geomechanical perspective with the injection of large amounts of CO<sub>2</sub>, which is required for a viable economic sequestration policy. In these scenarios, the injected CO<sub>2</sub> would likely result in a separate CO<sub>2</sub> phase because of excess CO<sub>2</sub> over the amount dissolved in water and oil. Additionally, many of the scenarios proposed have temperature (T) and pressure (P) conditions that would result in the presence of supercritical CO<sub>2</sub> (T >31°C and P >7.3 MPa). Due to the large amount of CO<sub>2</sub>, geochemical reactions will also play an important role, more than in typical enhanced oil recovery (EOR).

GS E&C and WorleyParsons have undertaken a collaborative research for conceptual modeling of CO<sub>2</sub> sequestration within the depleted Meruap oil reservoir in Indonesia (Chae 2015). This has been achieved by (a) providing the rationale for choosing a CO<sub>2</sub> sequestration modeling software from the wide variety of packages available worldwide, (b) providing a demonstration of CO<sub>2</sub> sequestration in a depleted oil reservoir, (c) exploring three common CO<sub>2</sub> leakage risk scenarios and (d) demonstrating a methodology of weak coupling of FEHM code (Finite Element Heat Mass, Zyvoloski 2003) with GoldSim for probabilistic risk analysis. The primary objective of this study is to simulate CO<sub>2</sub> injection and subsequent transport under different possible scenarios for the purpose of sequestration. We have used the FEHM to perform the simulations, including simulations of possible leakage pathways.

## **2. DEMONSTRATION OF FEHM CO<sub>2</sub> simulation CAPABILITY**

The most likely and most studied storage reservoirs are sedimentary in nature. They may or may not contain hydrocarbons, but often contain multiple permeable aquifers containing brine of varying concentration separated by confining units. The aquifer can be large, perhaps spanning a basin of 100 km in scale or small in extent, separated by sealing faults, of tens of meters to kilometers in scale. Such features and constructs often cross through shallower freshwater aquifers. Deeper aquifers are frequently more compartmentalized, and have little flow, geologically older water, and higher to much higher salinity. In hydrocarbon reservoirs, dense brine usually accompanies the hydrocarbons. The deeper aquifers or reservoirs with high brine concentrations are likely targets for CO<sub>2</sub> injection. The leakage scenarios demonstrated address the capacity, safety and monitoring issues associated with these types of settings.

This study is limited to three leakage scenarios: 1) leakage through a wellbore and annulus, 2) leakage through caprock and 3) leakage through a fault. Three-dimensional models are developed for these scenarios for the following reasons: Contrary to 2D model, 3D models allow for simulation of non-radial flow in wellbore models. Point sources that have 3D flow fields provide higher pressure gradients (more conservative) than 2D models. If one of the dimensions is averaged, even with uniform permeability, there will be localized pressure gradients that will be higher and lower in 3D. When transporting CO<sub>2</sub> (e.g. across a caprock) the breakthrough will always be earlier in 3D because of the localized higher gradients.

### *2.1 Conceptual Setting for Leakage Models*

#### *2.1.1 Wellbore Leakage model*

The wellbore leakage model simulates leakage through the annulus or through a cracked cement plug in a passive or retired well. These wells usually have a cement plug in the wellbore and annulus regions of often unknown competency. Their location in a long-abandoned oil field is often unknown. There are a number of simplified flow models for flow through the cement plug inside the well (Celia 2011). The numerical grid designed to examine the CO<sub>2</sub> leakage near a well and annulus is a relatively small scale cylindrical 3D model with about 100 m in diameter. Beside the plugged well, it includes the details of a typical annulus: wellbore-cement interface, cement and a cement-rock interface. The target aquifer for CO<sub>2</sub> storage, a confining layer (caprock) and a fresh water aquifer (above) are also included.

The model is shown in Figure 3 (a). The “well and annulus position” is a hypothetical existing passive or retired well screened in the reservoir (e.g. an abandoned oil well) that may provide a leakage pathway (i.e. a “leakage well”). The “injection point” (i.e. the actual injection well) was placed near the bottom of the leakage well to provide a conservative situation in which the injection well is located in close proximity to an abandoned well, for the sole purpose of generating a CO<sub>2</sub> plume and a high pressure region to facilitate flow in the complex annular region of the leaking well. The detail around the wellbore is magnified in Figure 3 (b). This grid is very high-resolution near the wellbore because of the steep pressure gradients and the necessity to represent leakage paths in that region (steel-cement interface; within cement; and cement-rock

interface). These leakage paths are susceptible to stress changes due to pumping or injection, chemical degradation due to high concentrations of dissolved CO<sub>2</sub>, impurities in the CO<sub>2</sub> itself, and age-related degradation in abandoned wells. The numerical mesh has 40,280 nodes and 38,480 brick (8 nodes) elements.

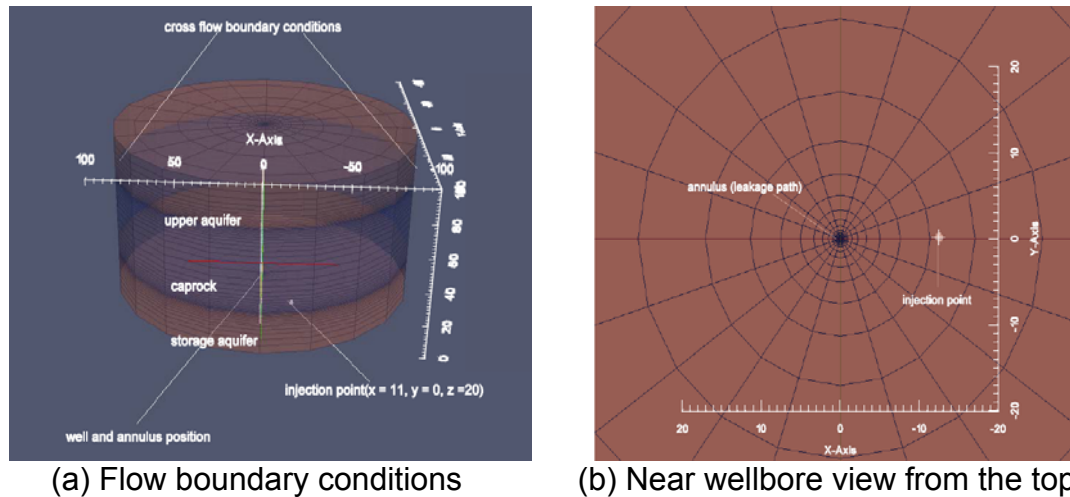


Fig. 3 Wellbore leakage model

Selected reservoir parameters and operational conditions based on assumed rock types and known values are provided in Table 1. Of note are the vertical permeabilities; they are considerably larger (smaller negative numbers in the exponent) than the horizontal values. These permeabilities represent cracks and connected pores that may be present in older or damaged wells. This model is considerably smaller in extent (100 m radius and 100 m depth) than the other two leakage models that represent kilometer size reservoirs. This model does not include a pressure-relief well in the storage aquifer. The small vertical extent (100 m) makes the constant temperature model a reasonable approximation. The 10°C temperature means the CO<sub>2</sub> transitions from liquid CO<sub>2</sub> to gaseous CO<sub>2</sub> as it travels from the storage aquifer to the upper aquifer.

Table 1 Reservoir Parameters and Injection Rate for Wellbore Leakage model

Parameter	Steel-cement	Cement	Cement-caprock	Storage aquifer	Upper aquifer	Caprock
Thickness (m)				25	25	50
Permeability (log m <sup>2</sup> )	-16	-15	-14	-13	-13	-22
Vertical permeability (log m <sup>2</sup> )	-12	-11	-11	-13	-13	-22
Porosity	0.1	0.1	0.2	0.25	0.25	0.1
Brine mass fraction	0.01	0.03	0.03	0.01	0.01	0.03
Injection rate (kg/s)				0.1		
Brine well impedance kg/ (s*MPa)				N/A		
Temperature	10°C	10°C	10°C	10°C	10°C	10°C

Note: 1 darcy  $\approx 10^{-12}$  m<sup>2</sup>

### 2.1.2 Caprock Leakage model

The caprock model (Figure 4) consists of two aquifers separated by a caprock. In a typical setting, the caprock would have relatively low permeability, but may also vary in thickness, with heterogeneous permeability and likely fracturing (or faulting) as well. In our conceptual model, permeability and thickness are assumed to be uniform. The caprock leakage model constructed is coarsely modeled (Ruqvist 2002), but it is 3D, rather than 2D. The third dimension allows for explicit representation of cross-formational groundwater flow (cross flow) in the upper aquifer, important for evaluating brine mixing, plume development (direction, extent and dilution) and for more accurate and conservative pressure computation than the corresponding 2D model. Cross flow is simulated by applying boundary conditions (specified fluid pressure) on the left and right sides of the models in the upper aquifer to establish a “natural groundwater flow” in that aquifer, which, in turn, interacts with the CO<sub>2</sub> plume. This allows a realistic context for observing dilution of a CO<sub>2</sub> leak from the storage aquifer, and would aid in the design of a monitoring system if the characteristics of the upper aquifer are known.

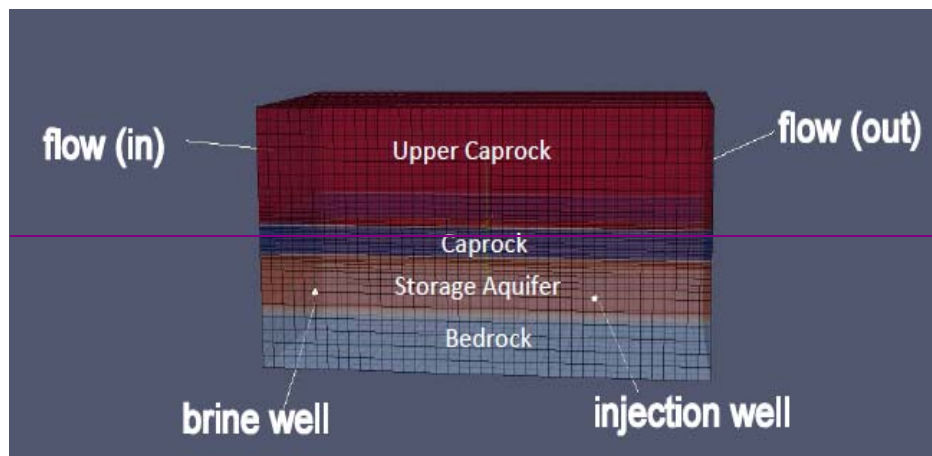


Fig. 4 Caprock leakage model and flow boundary condition

When injecting CO<sub>2</sub> for the purposes of CCS, a brine extraction well (“brine well” as shown in the figure) is often needed in order to relieve and attenuate pressures in the storage aquifer when large amounts of CO<sub>2</sub> are injected. These “brine wells” extract fluid from the storage aquifer while the CO<sub>2</sub> is injected, to maintain a safe pressure, which is needed when injecting into nearly incompressible liquids like water. In the scenario analyzed, the brine well thus is a relief well. The model assumes that the reservoir portion is filled mainly with brine, while being dedicated for CO<sub>2</sub> storage. The brine well would then be used to extract brine, to make room for more CO<sub>2</sub> (to be injected through the main well), and maintain a safe (non cracking) pressure in the injection reservoir. In an EOR operation, the brine well would likely be an old producing well with some small quantities of oil and CO<sub>2</sub> being produced together with the brine. The operation of the brine well would have different objectives in each case.

If an aquifer contains only brine and is for storage only and does not have producing wells such as an oil reservoir, then it is highly likely that brine wells will be needed to keep the pressure increase due to CO<sub>2</sub> injection in a safe range. If the reservoir is extremely large (good situation) or very leaky (bad situation) then brine wells may not

be important as the physical setting is likely conducive to keeping the pressure buildup safe. Therefore this is situation dependent.

The brine well for the caprock scenario extracts water at a rate (Q) sufficient to maintain a constant pressure:

$$Q = I \cdot (P_r - P_w) \quad (1)$$

where I is the impedance ( $2 \cdot \pi \cdot r_w \cdot K \cdot L / \gamma$ ),  $P_r$  is the reservoir pressure, and  $P_w$  is the well pressure ( $K$  is the aquifer hydraulic conductivity,  $r_w$  is the well radius, and  $L$  is the screen length). In the simulations I and  $P_w$  are input and remain constant. A very small I value indicates a very low brine extraction rate, Q, whereas a very large I value indicates that reservoir and well pressures are essentially equal. In practice, the operator would strive to have a high pressure at the brine well, so that less brine is removed, while preventing short-circuiting from injection well to the brine well that would result in less stored CO<sub>2</sub>. We note that the simulations were run with no salt. The salt concentrations are small and do not affect the results - viscosity and density of pure water are used.

As shown Figure, this model is used to examine the CO<sub>2</sub> leakage through a caprock with its uniform thickness and the placement of injection and pressure attenuation/relief (brine) wells. This geometry is similar to that found in many sedimentary sequences in typical oil and gas reservoirs. This model is 2 km long, 1 km wide, and is 1 km deep. Extra resolution is added near the interfaces between the different units: storage aquifer, upper aquifer, and caprock, due to the steep pressure gradients and the necessity to represent leakage paths in those regions. The numerical grid has 18,500 nodes and 16,000 elements.

Table 2 shows the parameter values based on assumed rock materials and associated published and used ranges. The ratio of vertical to horizontal permeability (1:10) is typical of sedimentary units. This model is useful for injectivity studies (flow rate vs. pressure) and mixing (CO<sub>2</sub> and brine) in the upper aquifer. With the applied parameters and boundary conditions, the groundwater flow rate in the upper aquifer is about  $2.0 \cdot 10^{-7}$  m/s.

**Table 2 Reservoir Parameters and Injection Rate for Caprock Leakage Model**

Parameter	Upper	Caprock	Storage	Bedrock
Thickness	450	100	200	250
Permeability (log m <sup>2</sup> )	-12	-18	-13	-16
Vertical permeability (log m <sup>2</sup> )	-13	-18	-14	-17
Porosity	0.3	0.1	0.2	0.05
Brine mass fraction	0.01	0.03	0.03	0.03
Injection rate (kg/s)			3	
Brine well impedance kg/(s*MPa)			1.e-3	
Temperature <sup>1</sup>	varies	varies	varies	varies

Note: <sup>1</sup> Temperature = 35° - 0.025 \* (z-500), 1 darcy ≈ 10<sup>-12</sup> m<sup>2</sup>

### 2.1.3 Fault Leakage model

The fault leakage model (Figure 5) is similar to the caprock leakage model and also consists of two aquifers separated by a caprock. The only addition to the caprock model is the fault. This allows for simulation of cross formational groundwater flow in the upper aquifer; for evaluating brine mixing based on simulated plume evolution; and more accurate pressure computations, compared with a corresponding 2D model.

As with the caprock leakage model, the model is 2 km long, 1 km wide, and is 1 km deep. In addition, a highly resolved fault is part of this grid (3,600 nodes). The model includes 22,099 nodes and 19,200 elements.

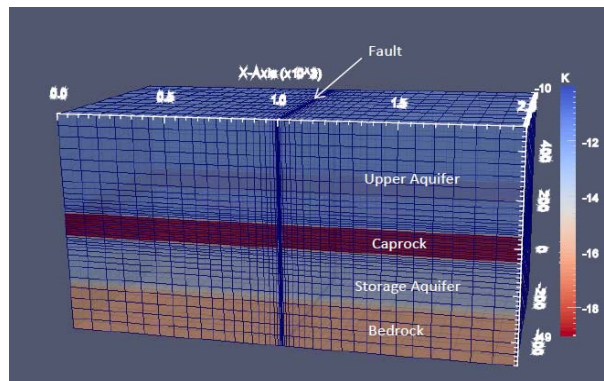


Fig. 5 Fault leakage model showing high resolution fault

Table 3 Reservoir Parameters and Injection Rate for Fault Leakage Model

Parameter	Upper	Caprock	Storage	Bedrock	Fault
Thickness (m)	450	100	200	250	
Permeability (log m <sup>2</sup> )	-12	-18	-13	-16	-10
Vertical Permeability(log m <sup>2</sup> )	-13	-18	-14	-17	-10
Porosity	0.3	0.1	0.2	0.05	0.5
Brine mass fraction	0.01	0.03	0.03	0.03	0.03
Injection rate (kg/s)			5		
Brine well impedance kg/(s*MPa)			1.e-3		
Temperature <sup>1</sup>	varies	varies	varies	varies	varies

Note: <sup>1</sup> Temperature = 35° - 0.025\*(z-500), 1 darcy ≈ 10<sup>-12</sup> m<sup>2</sup>

The simulation parameters are shown in Table 3, which was based on published values associated with assumed rock materials. The fault permeabilities are assigned as very high values relative to the adjacent rock due to the uncertainty in fault conductivity that normally exists, it is typically considered a random variable in a stochastic framework such as Monte Carlo Simulations for risk assessment purposes but only limited sensitivity analysis is conducted herein. The fault porosity was arbitrarily set to a high value of 0.5, assuming filling with highly porous fine materials. We note that the even with the extra resolution to represent the fault, the smallest grid-

block is about 1 m. Field observations commonly indicate width of minor faults to be less than 1 m.

#### 2.1.4 CO<sub>2</sub> Injection Scenarios and Boundary Conditions

There has been research done in both the sequestration communities and the oil industry regarding the injection of CO<sub>2</sub>. For CO<sub>2</sub> sequestration, the objectives are the storage of maximum amount of CO<sub>2</sub>, while preventing, or at least, minimizing the leakage of CO<sub>2</sub> and brine to surrounding aquifers. For EOR applications, the injected CO<sub>2</sub> is designed to maximize the mobility of previously bypassed oil, and minimize the cost of the operation. Any CO<sub>2</sub> that is not produced with the oil can be counted as stored. Reservoir pressures and temperatures play a very important role. Reservoirs with pressures below about 7 MPa would have CO<sub>2</sub> existing mostly as gas at normal to warm temperatures. Under such pressure, and temperatures above 31 °C, CO<sub>2</sub> exists at a supercritical state.

In general it is well known that supercritical state of CO<sub>2</sub> can be achieved at depths larger than 800 m. In the caprock and fault leakage problems, the thicknesses of the various hydrostratigraphic units are: upper aquifer 450 m, caprock 100 m, storage aquifer 200 m, and base/bedrock aquifer is 250 m, with a total vertical dimension of 1,000 m.

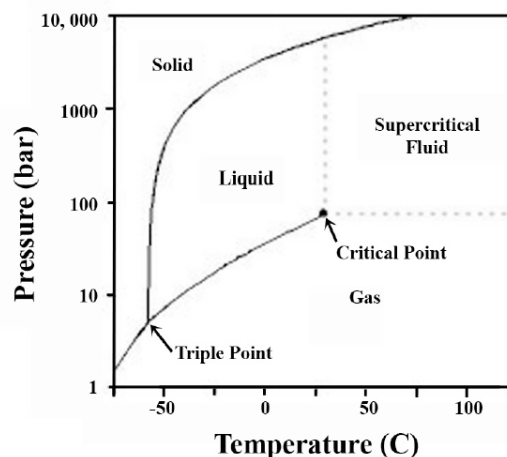


Fig. 6 CO<sub>2</sub> phase diagram (1 bar = 0.1 MPa)

Boundary conditions for the caprock and fault leakage problems are shown in Figure 7. The upper aquifer boundary pressure was about 5 MPa. This provided a pressure range of 5 - 15 MPa within the vertical profile. In addition, there were temperature variations from 22.5 °C to 72.5 °C along the vertical profile. The CO<sub>2</sub> phase states at different depths are also shown in the figure, with supercritical conditions existing in the reservoir.

There are two primary injection scenarios: 1) injection at a specified flow rate, and 2) injection at a specified pressure. In practice, injection is usually a combination of both types. CO<sub>2</sub> sequestration injection is usually as large as possible under the constraints of no fracture activation or seismicity. This puts a constraint on the maximum downhole

injection pressure. In many geologic settings, this maximum pressure is equal to the least principal stress, and is approximately half the lithostatic stress.

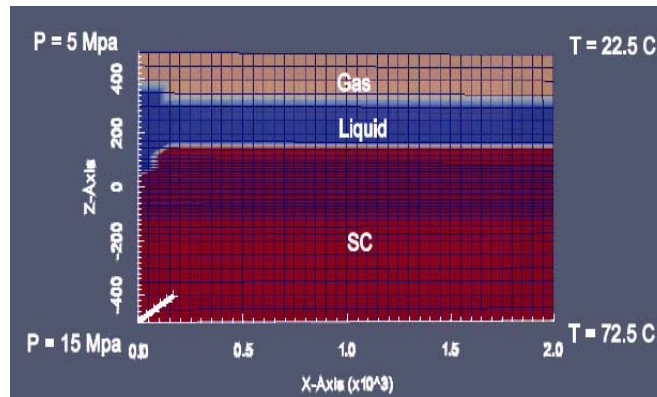


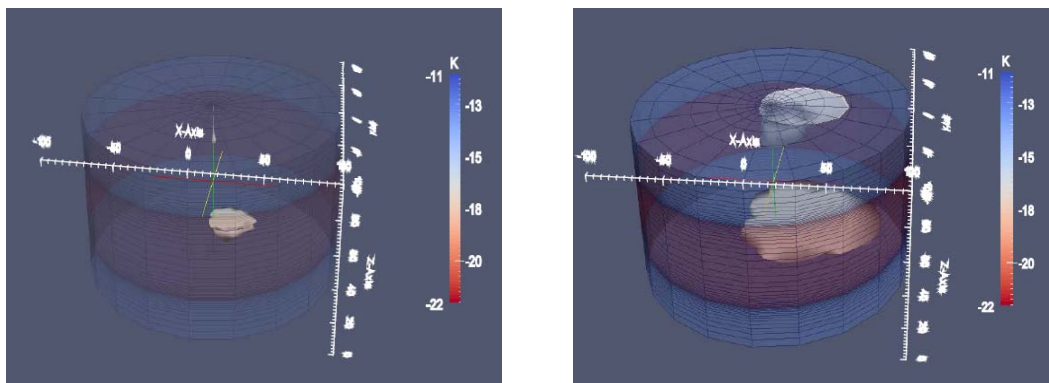
Fig. 7 CO<sub>2</sub> phase regions in subsurface with hydrostatic pressure and 0.05 °C/m temperature gradient

## 2.3 Simulation Results

### 2.3.1 Wellbore Leakage model

The example simulation chosen for the wellbore leakage problem focuses on CO<sub>2</sub> transport in and near the annulus of the leakage well. The injection is from a point source (injection well). Flow is in the annular region. The CO<sub>2</sub> injection is from a single source located about 6 m below the bottom of the caprock, and about 10 m horizontally from the abandoned leakage wellbore.

#### 2.3.1.1 Case 1



(a) After 20 days of injection

(b) After 100 days of injection

Fig. 8 CO<sub>2</sub> plume (Case 1\_Wellbore Leakage model)

Figure 8 (a) shows a CO<sub>2</sub> plume (CO<sub>2</sub> saturation of 1%) after 20 days of injecting of about 172,800 kg of CO<sub>2</sub> using the model input parameters. The 1 % CO<sub>2</sub> saturation shown is a convenient way to visualize the extent of the CO<sub>2</sub> plume. In large cells,

where the CO<sub>2</sub> saturations are averaged over large distances, this is useful but not an accurate way (because of numerical smearing) of visualizing the plume dimension. So long as we use the same criteria (i.e. 1 % CO<sub>2</sub> concentration in this case) we can compare different scenarios as is done by comparing to subsequent figures.

As can be seen in the figure, a small amount of CO<sub>2</sub> has reached the upper aquifer just above the caprock. The leakage path is mainly via the cement-caprock interface (highest permeability/least resistance) at the wellbore annulus of the leakage well, representing an old abandoned well in the vicinity of the injection well. Figure 8 (b) highlights the expansion and migration of the CO<sub>2</sub> plume (CO<sub>2</sub> saturation of 1%) after 100 days (864,000 kg CO<sub>2</sub> injected) in both the storage aquifer and the upper aquifer for Case 1. The figure shows that the plume growth in the storage aquifer is relatively circular and buoyancy has constrained it to the top of the storage aquifer. A small anomaly indicates that the leakage well has pierced the lower plume. The upper plume is shifted to the right because of the ambient groundwater flow (left to right) in the upper aquifer.

### 2.3.1.2 Case 2

The plume sensitivity to increasing permeability of the upper aquifer from 1E-13 to 1E-12 is illustrated in Figures 8. A close inspection of the difference between the plumes in Figures 8 and 9 shows only little difference. This is a result of two factors. First, the flow rate in the upper aquifer is constrained by boundary conditions to be the same in both scenarios, and second, the major resistance (inversely related to permeability times flow area) to migration of CO<sub>2</sub> in this multiple aquifer system is the annulus of leakage well. The lack of sensitivity therefore is a result of the flow resistance in the annulus being much larger than that of the upper aquifer.

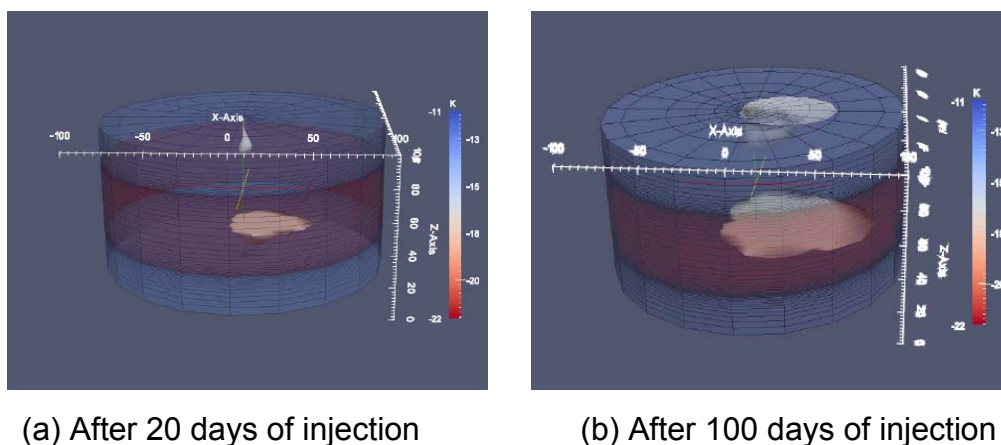


Fig. 9 CO<sub>2</sub> plume (Case 2\_Wellbore Leakage model)

### 2.3.2 Caprock Leakage model

This model is used to examine the CO<sub>2</sub> leakage through a caprock with uniform thickness and the placement of injection and pressure attenuation/relief (brine) wells. This geometry is similar to that found in many sedimentary sequences in typical oil and gas reservoirs. The example simulation for the caprock leakage model highlights the phase change behavior of the CO<sub>2</sub>, as well as the different CO<sub>2</sub> storage rates obtained

by including dissolution of CO<sub>2</sub> in water versus not including CO<sub>2</sub> dissolution. The injection well (modeled as a point source) is located in the storage aquifer 1,250 m from a brine extraction well that is used to attenuate the pressure in the storage aquifer. The maximum CO<sub>2</sub> dissolution in water is about 6% by mass. An interesting fact is that the CO<sub>2</sub> dissolution increases the density of water allowing it to settle of the bottom of an aquifer. A number of different sensitivities are explored with the caprock leakage model, as summarized in Table 4.

Table 4 Cases Considered for the Caprock Leakage model

Case	Sensitivity Explored
1	Table 2 parameters (base case)
2	Case 1 with storage aquifer permeability increased by a factor of 10
3	Case 2 with CO <sub>2</sub> injection rate increased to 5 kg/s.
4	Case 3 but without dissolution of CO <sub>2</sub> in water.
5	Case 1 except with 5 kg/s injection, no dissolution, and caprock permeability increased by a factor of 100.

#### 2.3.2.1 Case 1

Figure 10 (a) shows a FEHM simulation after 5,000 days (about 14 years) at an injection rate of 3 kg/sec ( $1.296 \times 10^9$  kg CO<sub>2</sub> injected) with CO<sub>2</sub> dissolution enabled (Case 1). Figure illustrates the importance of 3D simulation, with CO<sub>2</sub> first migrating preferentially upward due to buoyancy effects and then spreading laterally along the Caprock and storage aquifer interface in both the x- and y-direction.

#### 2.3.2.2 Case 2

Figure 10 (b) illustrates that increasing the storage aquifer permeability by a factor of 10 allows the buoyancy of the free CO<sub>2</sub> phase to facilitate CO<sub>2</sub> accumulation at top of the storage aquifer, leading to a flattening and spreading of the CO<sub>2</sub> plume (compare to Figure 10 (a)).

#### 2.3.2.3 Case 3

With a higher permeability in the storage aquifer, it is possible to increase the CO<sub>2</sub> injection rate. The plume for a 5 kg/sec injection rate ( $2.16 \times 10^9$  kg CO<sub>2</sub> injected) is shown in Figure 10 (c). The main difference between Case 2 and Case 3 is a higher CO<sub>2</sub> saturation near the injection well. Basically, the plume size is proportional to the injection rate.

#### 2.3.2.4 Case 4

Turning off the CO<sub>2</sub> dissolution allows the sensitivity to dissolution to be explored. With respect to simulation of CO<sub>2</sub> dissolution, the numerical formulation forces equilibrium. This in turn dissolves all the CO<sub>2</sub> until the saturation limit is achieved. Figure 10 (d) shows the same simulation that was presented in Figure 10 (c), but with no dissolution. The extra CO<sub>2</sub> that was previously dissolved now produces a larger

plume. Comparison of Figures 10 (c) and (d) therefore addresses fluid physics in miscible and immiscible state. Even with CO<sub>2</sub> dissolution in water, not all of it becomes dissolved, and part of it remains in a separate (immiscible) state. The CO<sub>2</sub> phase behavior as considered in the modeling was complex with CO<sub>2</sub> in a dissolved (miscible) state, immiscible CO<sub>2</sub>, and free supercritical CO<sub>2</sub>, and finally in the upper aquifer gaseous CO<sub>2</sub> and water (including CO<sub>2</sub> dissolved in water).

### 2.3.2.5 Case 5

The integrity of the caprock permeability is important for ensuring that the CO<sub>2</sub> remains sequestered in the storage aquifer. Cases 1 to 4 did not lead to any breakthrough of CO<sub>2</sub> in the upper aquifer during the simulation timeframe of 5,000 days. Escape from the storage aquifer is sensitive to caprock permeability. Figure 10 (e) shows the effect of increasing the caprock permeability by two orders of magnitude. It should be noted that even with this increase, the caprock permeability is still three orders of magnitude smaller than that of the storage aquifer. Note the broad plume in both the storage aquifer (supercritical CO<sub>2</sub>) and the upper aquifer (gaseous CO<sub>2</sub>).

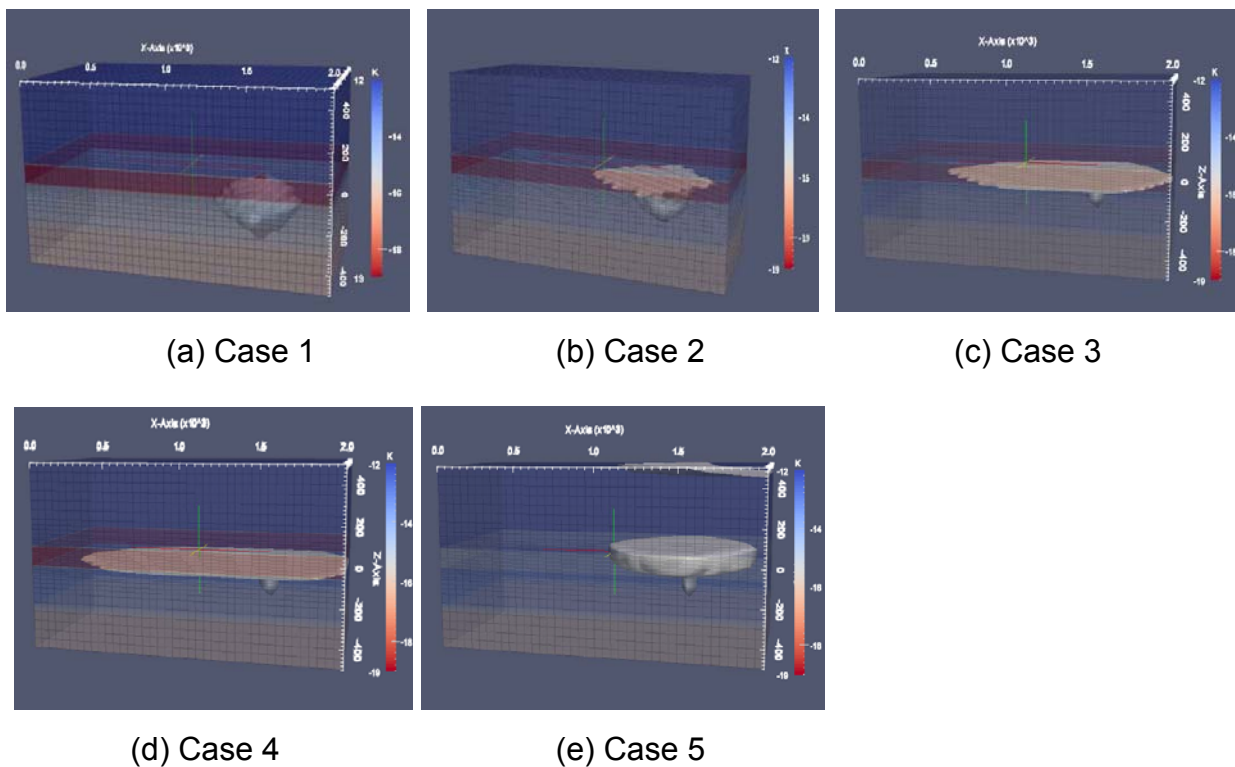


Fig. 10 CO<sub>2</sub> plume (Caprock Leakage model)

### 2.3.3 Fault Leakage model

Faults are common occurrence in potential storage reservoirs. Besides injectivity and mixing, the sensitivity to fault permeability (often unknown) can also be studied. A number of different sensitivities are explored with the fault leakage model, as summarized in Table 5.

### 2.3.3.1 Case 1

Figure 11 (a) shows a simulation result using the same injection rates and boundary conditions as the caprock model with the only addition of a fault with properties. The Figure shows two sheet-like plumes at the top of the storage and upper aquifers. The simulated CO<sub>2</sub> plume travelled to the fault and then, by buoyancy and forced convection, quickly reached the upper aquifer. While migrating through the fault, the CO<sub>2</sub> changed from a super critical to a gaseous state

Table 5 Cases Considered for the Fault Leakage model

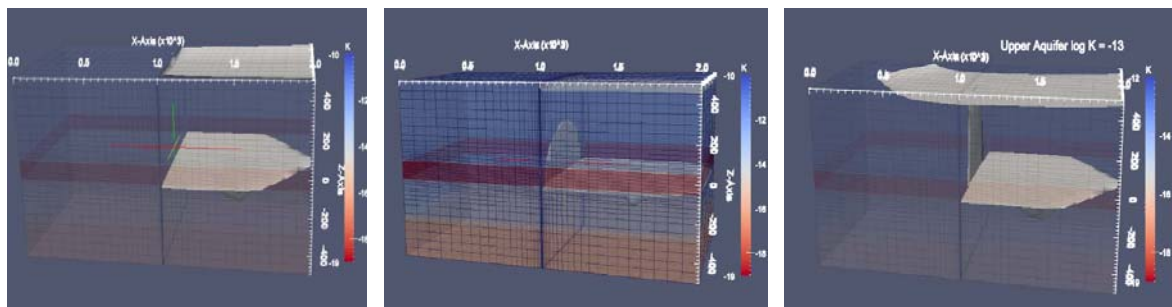
Case	Sensitivity Explored
1	Table 3 parameters (base case)
2	Case 1 with fault permeability decreased by a factor of 100
3	Case 1 with upper aquifer permeability decreased by a factor of 10

### 2.3.3.2 Case 2

In most reservoirs, injection and production of fluids are sensitive to fault permeability. Figure 11 (b) shows the CO<sub>2</sub> plume with a fault with two orders of magnitude smaller permeability than that listed in Table 3. In this figure, the plume is visible in the fault.

### 2.3.3.3 Case 3

Figure 11 (c) shows the CO<sub>2</sub> plume when the upper aquifer permeability was decreased by a factor of ten. This had a twofold effect; first, the cross-formational groundwater flow was reduced as the boundary conditions that produced the cross flow were constant pressure specified on the left and right sides of the upper aquifer; and second, flow resistance in the coupled aquifer system was changed. Figure 11 (c) shows this complexity as the plume is not predicted to move up-gradient (i.e. against the ambient cross formational flow direction) as well as down gradient.



(a) Case 1

(b) Case 2

(c) Case 3

Fig. 11 CO<sub>2</sub> plume (Fault Leakage model)

This example illustrates the importance of knowledge of properties of shallow aquifers for determining appropriate locations to monitor for potential breakthrough of CO<sub>2</sub>. Some indication of potential measurement differences is given in Figure 12. In the

figure, two time series of CO<sub>2</sub> content (equivalent to water or gas saturation) are compared for the two FEHM runs where the upper aquifer permeability was varied. The collection point is near the top center of the fault. Thus, while the lower permeability cases shows a somewhat broader plume, the higher permeability case delivers more CO<sub>2</sub> to the upper aquifer (smaller water saturation).

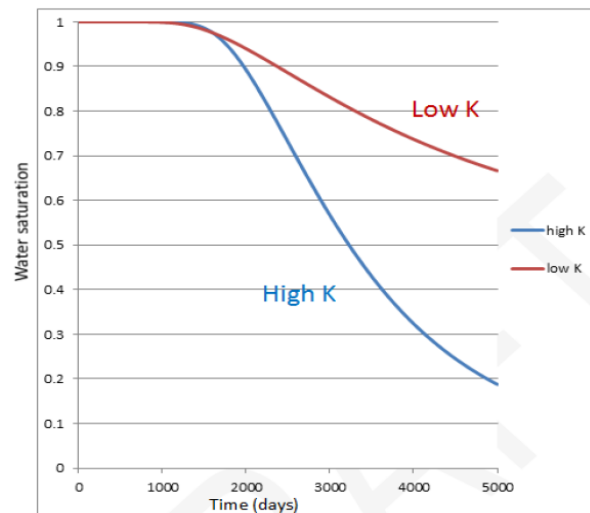


Fig. 12 Water saturation change for different upper aquifer permeability

#### 2.4 Summary of Analysis

The demonstrated CO<sub>2</sub> leakage models were presented with the primary focus of demonstrating FEHM software capability for this purpose. As discussed in previous sections, sensitivity analyses were an integral part of the simulations, showing a spectrum of sensitivities to the relevant parameters. In particular, the following sensitivities were evaluated for pressure buildup in the storage aquifer and CO<sub>2</sub> and brine leakage:

- Porosity of the storage formation;
- Permeability of the storage formation;
- Permeability of the caprock;
- Injection rate;
- Volume of storage formation; and
- Permeability of the upper aquifer.

It was demonstrated through the examples provided that rapid breakthrough of CO<sub>2</sub> to a shallow aquifer may occur through leaking wellbores (e.g. old oil wells). Faults were demonstrated to also be an important risk factor for potential leakage of CO<sub>2</sub> to a shallow aquifer overlying the storage aquifer. Areas where the caprock is thin and/or of greater permeability could also result in CO<sub>2</sub> leakage. It was further demonstrated that knowledge of the shallow (receiving) aquifer properties, flow regime, and buoyancy effects are important for proper location of monitoring points to assess potential breakthrough of CO<sub>2</sub>. Porosity and permeability of the storage aquifers and CO<sub>2</sub> dissolution were shown to be important controls on the amount of CO<sub>2</sub> that can be stored.

### **3. FEHM-GoldSim Coupling of CO<sub>2</sub> Sequestration**

In this section we show how GoldSim can be used in conjunction with FEHM so that CO<sub>2</sub> storage and leakage calculations can be performed probabilistically. GoldSim is general purpose probabilistic simulation software which has been used extensively for environmental modeling since its inception over two decades ago. In this study, GoldSim is used only in Monte Carlo simulation mode, to examine the effect of uncertainty in the parameters on the CO<sub>2</sub> sequestration operation. For CCS simulation purposes, the following GoldSim models have been developed for previous studies, illustrating example applications of probabilistic (risk) analysis.

#### *3.1 GoldSim – FEHM Coupling*

The method of coupling FEHM to GoldSim is to generate a response surface (Morgan 1990) in FEHM, which is a table of FEHM output values arranged in a table, against FEHM inputs. The table forms a set of grid points where FEHM outputs (responding to different inputs) are evaluated as a function of discrete inputs. GoldSim then calculates FEHM outputs for any intermediate (untested) input value by interpolating between known output values. In other words, the set of outputs resulting from different inputs (e.g. different parameter values) span a “space” of outputs as a function of any arbitrary set of input values contained within the space spanned these inputs, in all grid of points, and over time. In order to predict results for an input not included in the simulations, one could interpolate between two adjacent input-output pairs, and this is done for all grid points.

#### *3.2 Demonstration of GoldSim – FEHM Coupling*

##### *3.2.1 Reservoir Storage Capacity Example – Conceptual Model*

When designing a CCS system, there are many risks and uncertainties to consider. For example, the Wabamun Area Sequestration Project (WASP) was concerned with the feasibility of storing 1Gt of CO<sub>2</sub> in central Alberta, Canada (McGoey-Smith 2010). In WASP, the storage reservoir formation permeability, CO<sub>2</sub>-rock compressibility, storage reservoir porosity and abandoned well permeabilities were all uncertain and characterized by probability distribution functions. A GoldSim model was constructed to predict leakage from abandoned wells which is a major limitation for storing CO<sub>2</sub> in Alberta because of oil and gas activity.

In general for any storage reservoir, the storage capacity is dependent on the reservoir permeability and caprock permeability. Given that both permeabilities are uncertain, the storage capacity will be uncertain. In risk assessment, uncertain variables are quantified in terms of probability distribution functions (Bedford 2001). From knowledge of the probability distributions of the permeabilities it is possible to calculate the probability distribution of the storage capacity using the Monte Carlo method. GoldSim can be used as the Monte Carlo framework, and FEHM can be used as the engine to compute storage volume as a function of the permeabilities.

##### *3.2.2 Problem Implementation and Results*

To demonstrate the integrated FEHM-GoldSim modeling, we used a 5x5 table of points in this study to investigate the uncertainty in storage capacity of the aquifer as a function of uncertain aquifer permeability and uncertain caprock permeability using the response surface method. The model utilized is the caprock leakage model with identical numerical grid, parameters and boundary conditions. For the purpose of the Goldsim analysis, only the aquifer permeability and caprock permeability were varied from values. Note that equivalently, we could do the same to assess uncertainty (variability) in potential CO<sub>2</sub> leakage rates as a function of uncertain fault or caprock, or abandoned well annulus permeability.

The matrix of inputs and outputs for the storage capacity case is shown in Table 6, where  $k_{sa}$  is the permeability of the storage aquifer and  $k_{capr}$  is the permeability of the caprock. This matrix of inputs spans the range of storage aquifer permeability (first row) from lowest to highest possible values, and similarly for caprock permeability (first column). All other values in the matrix are the resulting outputs of storage capacity values. The storage capacity values were obtained by running FEHM for each of the combinations of storage aquifer permeability and caprock permeability and analyzing the FEHM output (results) for storage capacity. The storage capacity was calculated as the amount of CO<sub>2</sub> injected. The injection was constrained to keep the storage reservoir pressure under the fracture extension pressure (assumed as half the lithostatic pressure).

Table 6 Matrix of Storage Capacity Values (kg) as a Function of Storage Aquifer and Caprock Permeability (1 darcy  $\approx 10^{-12}$  m<sup>2</sup>)

Caprock Permeability $k_{capr}$ (m <sup>2</sup> )	Storage Aquifer Permeability $k_{sa}$ (m <sup>2</sup> )				
	1.00E-12	5.00E-13	1.00E-13	5.00E-14	1.00E-14
1.00E-18	9.44E+09	9.33E+09	8.70E+09	7.94E+09	4.34E+09
1.00E-17	9.51E+09	9.40E+09	8.78E+09	8.00E+09	4.39E+09
5.00E-17	1.01E+10	1.00E+10	9.36E+09	8.56E+09	4.82E+09
1.00E-16	1.10E+10	1.09E+10	1.01E+10	9.27E+09	5.33E+09
1.00E-15	4.65E+10	4.27E+10	3.06E+10	2.57E+10	1.39E+10

In general, higher permeability leads to higher CO<sub>2</sub> storage when injecting at a constant pressure. This not only goes for aquifer permeability but also for caprock permeability. That is, the greater the caprock permeability, the more CO<sub>2</sub> migrating from the storage aquifer into the caprock, hence the larger is the apparent storage in the storage aquifer (calculated as amount of CO<sub>2</sub> injected). The caprock does not leak until CO<sub>2</sub> reaches the upper aquifer. So some credit could be taken for a thick or permeable caprock in terms of overall CO<sub>2</sub> storage capacity and this is reflected in Table. Obviously this example does not account for the increased risk of CO<sub>2</sub> leakage associated with increased caprock permeability.

The two-dimensional probability distribution (hyper-surface; lookup table) of storage capacity allows us to perform a risk calculation on whether we have a large enough storage capacity to meet the storage needs for CCS. Next, a risk analysis is performed in Goldsim on the information from Table 6. Risk is defined as a triplet: it is a measure of the probability and consequences of an adverse event, given the presence of a hazard. The risk scenario here is that there will be insufficient storage for the mass of CO<sub>2</sub> we wish to sequester. The drivers of risk are the uncertainties in storage aquifer permeability and caprock permeability. The two input variables are modeled as triangular distribution functions which comprise three values: a lowest value, a highest value and a most likely value. Triangular distributions are used where there is a central tendency but with the possibility of skewing (asymmetric shape). They are commonly used in risk assessment and operations research. Here the upper and lower values of permeability were taken from minimum and maximum values from Table 6, and the most likely value of permeability estimated as the geometric mean of the upper and lower values.

We can now perform risk analysis on the GoldSim-FEHM simulator outputs. Because the inputs to the simulation are uncertain, in this case the two permeability parameters, the output from the simulation is also uncertain. The output is the histogram, or PDF (Probability Density Function) of CO<sub>2</sub> storage mass which the storage aquifer can support. If we need to store 20 million tones of CO<sub>2</sub>, then we can extract the probability that this condition can be met by typing in 2.0 E+7 into the left most box under the CDF (cumulative distribution function) plot in Figure 13. GoldSim estimates the probability of meeting this condition as 80.2%. Therefore we can say that the probability that the CO<sub>2</sub> storage (sequestration) system can meet a target volume of 20 Megatons is 80.2%.

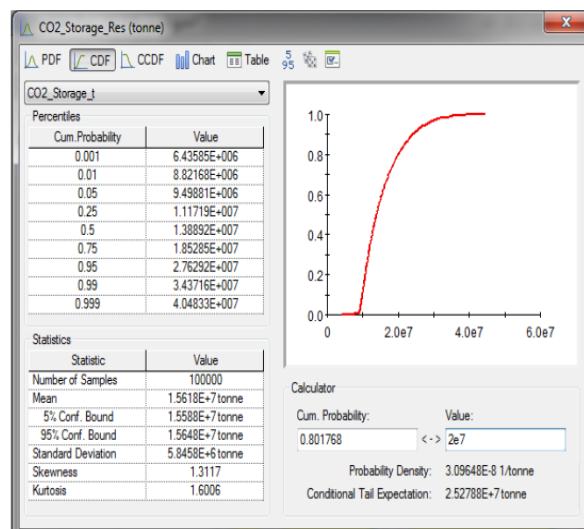


Fig. 13 GoldSim-FEHM outputs (histogram of mass in storage reservoir)

## **4. Conclusions**

The simulations presented in this paper demonstrated that FEHM can efficiently simulate important CO<sub>2</sub> leakage scenarios. Its ability to assist with the design of monitoring systems was demonstrated by time history plots of CO<sub>2</sub> saturation at key potential monitoring locations. All of the simulations were 3D; included cross-formational groundwater flow in the upper aquifer to represent natural aquifer conditions; included mixed miscible and immiscible states, dynamically; accounted for mixing and dissolution; and had the ability to simulate point sources to accurately simulate pressure buildup. The CO<sub>2</sub> phase behavior as considered in the modeling was complex with CO<sub>2</sub> in a dissolved (miscible) state, immiscible CO<sub>2</sub> and free supercritical CO<sub>2</sub>, and finally, in the upper aquifer gaseous CO<sub>2</sub> and water (CO<sub>2</sub> dissolved in water).

It is the authors' opinion that 3D models are necessary for almost all CO<sub>2</sub> injection studies because of the importance to model correct pressure responses. This would be amplified when incorporating/linking geomechanics and geochemistry in the model. Two-dimensional models are prone to underestimating the pressure response to injection, and may not represent the system well, even just for the purpose of sensitivity analysis.

The coupling of FEHM and the GoldSim package was demonstrated using the response surface (interpolation) approach. The successful coupling FEHM to GoldSim for the case of analyzing CO<sub>2</sub> storage capacity as function of storage aquifer permeability and caprock permeability demonstrated that probabilistic calculations can be carried out in future quantitative risk assessment work for other cases, including CO<sub>2</sub> leakage cases under uncertain parameters for caprock, faults or leakage wells.

## **Acknowledgement**

This study was supported by "The development of CO<sub>2</sub> geological storage technologies through 1,000 ton CO<sub>2</sub>-EOR pilot test" of the Korea Institute of Energy Technology Evaluation and Planning (KETEP) grant funded by the Ministry of Trade, Industry and Energy (MOTIE) (No. 2012T100201728)

## REFERENCES

- Bedford, T, and Cooke, R. (2001), "Probabilistic Risk Analysis: Foundations and Methods", Cambridge University Press, Cambridge, UK, 2001.
- Celia, M.A., Nordbotten, J.M., Court, B, Dobossy, M., and Bachu, S. (2011), "Field-scale application of a semi-analytical model for estimation of CO<sub>2</sub> and brine leakage along old wells." *International Journal of Greenhouse Gas Control* 5, **No. 2**, 257-269.
- Chae, K.S., Park, J.H., Lee, J.W., Orr, S. and Zyvolosk, G. (2015), "Analysis of Carbon Dioxide Storage and Potential Leakage Risks", the Korea CCS Int. Conference, Jeju, Korea.
- McGoey-Smith, A.D., Voss. C., and Heal, K.(2010), "Wabamun Area Sequestration Project: Risk-based Leakage Model", University of Calgary, January, 2010
- Morgan, M.G., and Henrion, M.(1990), "Uncertainty: A Guide to Dealing with Uncertainty in Risk and Policy Analysis", Cambridge University Press, Cambridge, UK, 1990.
- Rutqvist, J., and Tsang, C.-F.(2002), "A study of caprock hydromechanical changes associated with CO<sub>2</sub>-injection into a brine formation." *Environmental Geology* 42, **No. 2-3** 296-305.
- Rutqvist, J., Wu, Y.-S., Tsang, C.-F., and Bodvarsson, G., 2002. A Modeling Approach for Analysis of Coupled Multiphase Fluid Flow, Heat Transfer, and Deformation in Fractured Porous Rock. *Int. J. Rock Mech. & Min. Sci.* **39**, 429-442.
- Sharma, S., Cook. P., Berly. T., and Lees, M.(2009), "The CO<sub>2</sub>CRC Otway Project: Overcoming challenges from planning to execution of Australia's first CCS project" *Energy procedia* 1, **No.1**, 1965-1972.
- Zyvoloski, G.A., Robinson, B.A., and Viswanathan, H.S.(2008), "Generalized dual porosity: A numerical method for representing spatially variable sub-grid scale processes", *Advances in water resources* 31, **No.3**, 535-544.